



Pollen-recorded bioclimatic variations of the last ~22,600 years retrieved from Achit Nuur core in the western Mongolian Plateau



Aizhi Sun^{a,*}, Zhaodong Feng^b, Min Ran^c, Chengjun Zhang^d

^aKey Laboratory of Cenozoic Geology and Environment, Institute of Geology and Geophysics, Chinese Academy of Sciences, Beitucheng Western Road, Chaoyang District, Beijing 100029, China

^bXinjiang Institute of Ecology and Geography, Chinese Academy of Sciences, Urumqi 830011, China

^cMOE Key Laboratory of Oasis Ecology, College of Resources and Environmental Sciences, Xinjiang University, Urumqi 830046, China

^dCollege of Resources and Environmental Sciences, Lanzhou University, Lanzhou 730000, China

ARTICLE INFO

Article history:

Available online 23 July 2013

ABSTRACT

This research focuses on the reconstructions of vegetation variations and the associated climate changes over the past ~22,600 years based on pollen data of 91 samples obtained from Achit Nuur in the western part of the Mongolian Plateau. The vegetation in the Achit Nuur area was forests in higher elevations and steppes in lower elevations from ~22,600 to ~13,200 cal BP. The subsequent period from ~13,200 to ~6400 cal BP was characterized by steppes in higher elevations and deserts in lower elevations, followed by taiga expansion in high elevations in the following period from ~6400 to ~1600 cal BP. The last ~1600 years were characterized by high herb percentages. Pollen-based reconstruction of the temperature showed that the Achit area experienced cold conditions between ~22,600 and ~13,200 cal BP and mild conditions from ~13,200–~6400 cal BP with the past ~5000 years being relatively warm. The reconstructed precipitation suggests two wet periods: (1) from ~22,600 to ~13,200 cal BP and (2) from ~6400 to ~1600 cal BP. The two intervening dry periods are (1) from ~13,200–~6400 cal BP and (2) from ~1600 to 0 cal BP.

© 2013 Elsevier Ltd and INQUA. All rights reserved.

1. Introduction

The western Mongolian Plateau where the study site (i.e., Achit Nuur) is situated is an important climatic conjunction between the Pacific-influenced climates and the Atlantic-influenced climates. Many palaeoenvironmental studies, mostly on the basis of radiocarbon-dated sedimentary records from lakes, were conducted in this region and surrounding regions (e.g., Altai Mountains, northern and central Mongolian Plateau, northern China Xinjiang region) and have been published during the past twenty years (e.g., Harrison et al., 1996; Tarasov et al., 1998, 2000; Gunin, 1999; Grunert et al., 2000; Rudaya et al., 2009). However, discrepancies are more pronounced than consistencies regarding the Holocene climate change sequences in this region and three controversies are relevant to this study focusing on a Holocene record from Achit Nuur in the western Mongolian Plateau. Group one claims that the western Mongolian Plateau has been primarily influenced by the East Asian Monsoon during the Holocene and

that influence was at its maximum during the mid-Holocene Climatic Optimum (Harrison et al., 1996; Tarasov et al., 2000). Group two states that the entire Central Asian Arid Zone (CAAZ) that stretches from the Caspian Sea in the west to the Hinggan Mountains in the east and that includes the western Mongolian Plateau has been climatically controlled by the North Atlantic Ocean and experienced the Holocene moisture changes that was out-phased with that in monsoon-dominated China (Chen et al., 2008). Group three proposes that the Holocene moisture variations in the arid and hyper-arid Mongolian Plateau including the western Mongolian Plateau has been primarily modulated by the temperature and that the mid-Holocene was the driest interval under warmest climate (Wang et al., 2009, 2011; Wang and Feng, 2013). These palaeoclimatological controversies call for more high-resolution palaeoclimatic reconstructions from the entire Mongolian Plateau.

This paper presents a record of environmental variations and the associated vegetation changes based on 91 pollen samples and 10 ¹⁴C dates from a 200 cm lake core at Achit Nuur (49°25'N, 90°31'E) (Fig. 1) in hope the preliminary reconstruction by Gunin (1999) that was based on only four radiocarbon dates and only twenty pollen samples can be significantly improved for furthering our understanding of regional climatic variations.

* Corresponding author.

E-mail addresses: sunaizhi@mail.iggcas.ac.cn (A. Sun), fengzd@xju.edu.cn (Z. Feng).

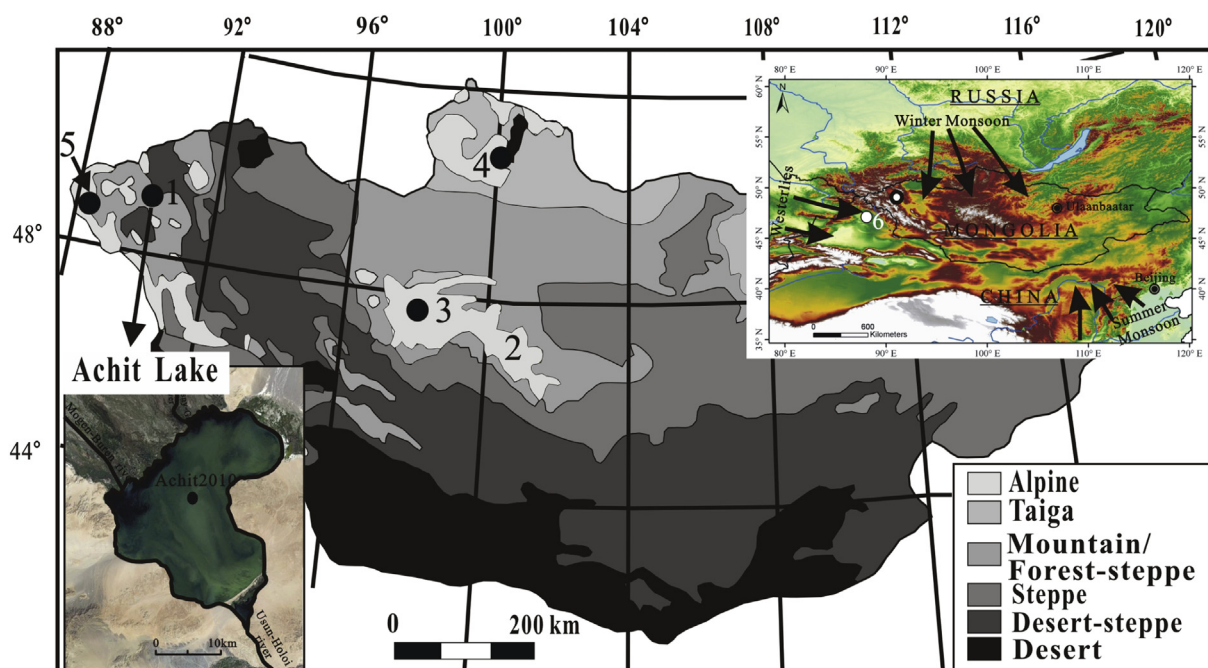


Fig. 1. Location and settings. A. Location of Achit Nuur (site 1) and other sections mentioned in the text (2: Ugiu Nuur; 3: Telman Lake; 4: Hovsgol Lake; 5: Hoton Nuur; 6: Wulungu Lake). B. Vegetation map of the Mongolia region (Hilbig, 1995). C. Map of Achit Nuur showing the location of sediment core (from <http://maps.google.com>).

2. Regional setting

Achit Nuur (49°25'N, 90°31'E, 1444 ± 5 m), a large fresh-water lake, is located in the intermountain basin surrounded by Mongolian Altai Mountains in the west, Mungen Taiga Mountain in the north and Kaharkhiraa–Turgen Mountain in the east (Fig. 1B). The lake has an area of 297 km². The maximum length is 24 km and the maximum width is 18 km, and the average depth is ca. 2 m and the maximum depth is ca 5 m. This freshwater lake has inflows from the Huv-Usny-Gol River and the Mogen-Buren River and has an outflow through the Usun-Holoi into the Kobdo River, the Kobdo River flowing into the closed Hara-Us-Nuur Lake.

The climate around Achit Nuur is characterized by long, cold, dry winters and short, cool, relatively wet summers. Mean temperatures vary between –16 and –21 °C in January and between 15 and 20 °C in July. Mean annual precipitation (MAP) ranges between 200 and 300 mm in the lake area. The Achit Nuur basin has low-lying swampy northern and southern shores covered with salt-marsh vegetation and high-ground eastern and western shores covered with desert steppe vegetation. The regional vegetation is dominated by species of *Stipa krylovii*, *Stipa gobica*, and *Cleistogenes soongorica*, mixed with shrubs of *Artemisia frigida*, *Artemisia xerophytica*, *Artemisia caespitosa*, *Tanacetum sibiricum*, *Tanacetum achillaeoides*, and *Tanacetum trifidum*. Macrophyte vegetation (*Chara* and *Potamogeton*) is widespread in the shallow zone (Hilbig, 1995). It should be mentioned that mountain taiga vegetation, dominated by *Larix sibirica* and *Pinus sibirica*, is distributed mainly in the Mongolian Altai Mountain and that the associated shrub layer includes *Rosa acicularis* and *Betula rotundifolia*. The forest-steppe vegetation borders the mountain taiga zone to the north and the steppe and desert-steppe zones to the south.

3. Materials and methods

3.1. Core collection and non-pollen proxy measurements

A 2.0-m-long sediment core was collected with a Livingstone-type gravitational piston corer in August of 2010 in the central

part of Achit Nuur where the water depth is 3.8 m. The core was cut longitudinally into two halves and visually described immediately after core retrieval in the field.

The grain size was measured at 2-cm intervals using a Malvern Co. Ltd. Mastersizer 2000 laser diffraction particle size analyzer (size range 0.02–2000 μm). Sample pretreatment included: (1) adding H₂O₂ to remove organic matter and soluble salts, (2) using diluted 1 N HCl to remove carbonate and (3) using Na-hexametaphosphate to disperse aggregates. Total organic matter content (TOC) was determined at 2 cm intervals using the anti-titration method with concentrated sulfuric acid (H₂SO₄) and potassium dichromate (K₂Cr₂O₇). All of the aforementioned analyses were conducted in the MOE Key Laboratory of Western China's Environmental Systems at Lanzhou University.

The core can be stratigraphically divided into five units primarily according to the organic matter content (OM) and the mean grain size (Fig. 2A). Sediment Unit 1 (200–165 cm) is a light-grey clay layer with a mean grain size of ~5 μm and an average organic matter content (OM) of ~2.5%. Sediment Unit 2 (165–150 cm) is a dark-colored silt or fine sand layer with a mean grain size of ~120 μm and an average organic matter content of ~5%. Sediment Unit 3 (150–130 cm) is a light-grey silt layer with a mean grain size of ~18 μm and an average organic matter content (OM) of ~7.5%. Sediment Unit 4 (130–112 cm) is a brownish-grey layer with a mean grain size of ~90 μm and an average organic matter content of ~5%. Sediment Unit 5 (112–0 cm) is a laminated and dark-colored silt with two interbedded sandy silt layers (i.e., 112–105 cm and 62–52 cm). Compared with the underlying Sediment Unit 4, Sediment Unit 5 has a higher OM (~10%) and a lower mean grain size (~22 μm).

3.2. Dating and age-depth model

Ten samples of bulk sediment were radiocarbon dated using accelerator mass spectrometry (AMS) at the NSF-AMS Facility at the University of Arizona (Table 1). To assess the carbon reservoir effect, we obtained an age of 2099 ¹⁴C BP on the bulk sediment

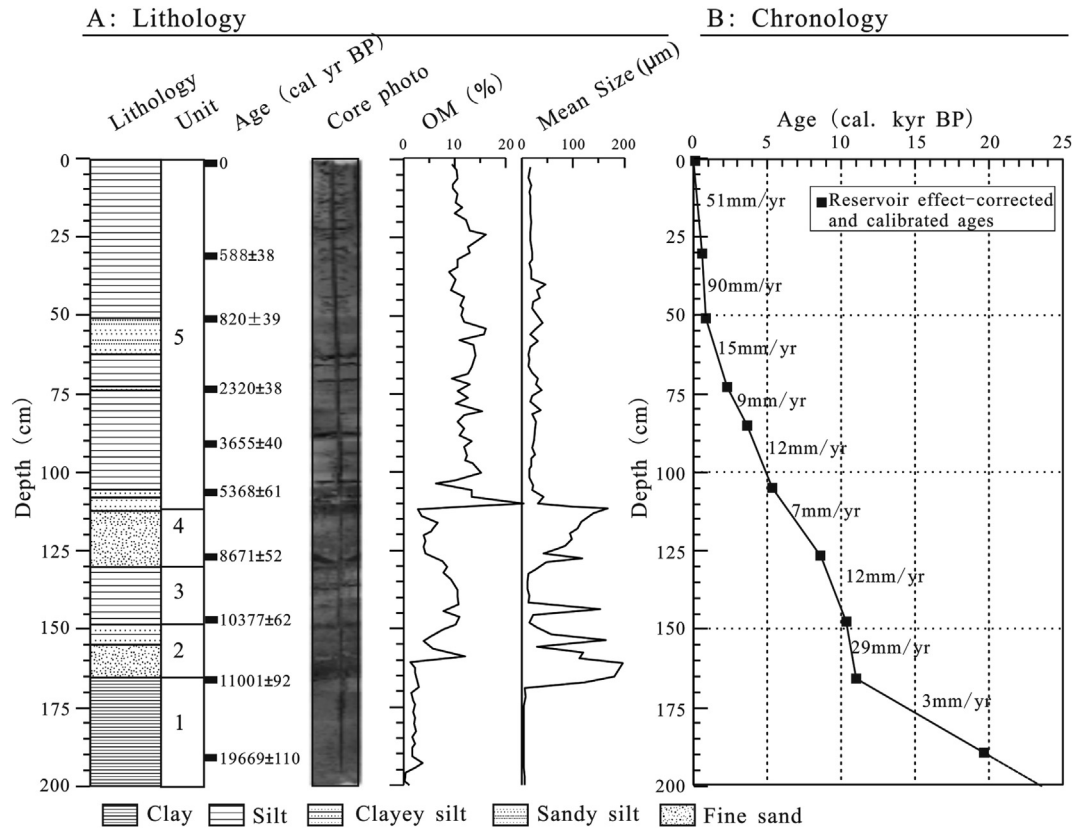


Fig. 2. Lithology, core photo, OM (%), Mean Grain Size (μm), and age-depth model of Achit Nuur core.

sampled at 0–2 cm (see Table 1). To account for the reservoir effect for the entire core, 2100 years were subtracted from all original ^{14}C ages assuming that it is constant through the core, and then all dates were calibrated to calendar years before present (BP = 1950 AD) with the program CALIB 6.0 using the INTCAL 09 calibration dataset (Reimer et al., 2009). The age-depth model was established based on a linear relationship between the depths and dates. Ages older than 19500 cal BP were extrapolated from the age-depth model between 165 cm and 190 cm in depth (Fig. 2). The age-depth model indicates that the upper 200 cm of the Achit Nuur core sediment covers the last ca. 22,600 years. The estimated depositional rates are ranged from 3 mm/y to 90 mm/y at whole core sediment. Calibrated radiocarbon ages are used throughout the paper.

Table 1
Dating results of Achit Nuur core.

LAB code	Depth/cm	Dated material	$\delta^{13}\text{C}$ (‰)	^{14}C age (yr BP)	Calibrated age after subtracting the reservoir effect (2σ) (cal BP)
AA94349	0–2	Bulk sediment	-13.3	2099 ± 35	0
AA94350	30–31	Bulk sediment	-13.0	2673 ± 38	524–652
AA94351	51–52	Bulk sediment	-11.7	2981 ± 39	725–926
AA94352	73–74	Mollusc	-8.3	4421 ± 38	2180–2460
AA94353	85–86	Bulk sediment	-9.0	5497 ± 40	3488–3823
AA94354	105–106	Bulk sediment	-7.9	6717 ± 61	5258–5478
AA94355	127–128	Root	-7.9	9971 ± 52	8547–8795
AA94356	148–149	Bulk sediment	-7.6	11300 ± 62	10235–10519
AA94357	165–167	Bulk sediment	-6.9	11796 ± 92	10755–11247
AA94358	190–191	Bulk sediment	-3.7	18600 ± 110	19463–19875

3.3. Pollen analysis and pollen indices

Totally, 91 pollen samples were obtained at 2–4 cm intervals from the sediment core. For pollen analysis, a tablet of *Lycopodium* (containing $27,637 \pm 563$ spores) was first added for calculation of pollen concentration (Moore et al., 1991). The fossil pollen samples were first treated with HCl (5–10%) and HF (36%) and sieved in ultrasonic bath. Pollen types were identified using pollen references including pollen books and photographs (Erdtman, 1978; Moore and Web, 1987; Wang et al., 1995) and our own type-slide collection of more than 200 plant species from northern China. The treated samples then were mounted and examined with a transmitted light microscope (Olympus BX 51) at $400\times$ magnification. More than 300 pollen grains (not including spores) were counted for each one of the samples. The percentage of each pollen type was calculated based on the sum of all counted pollen grains and the pollen diagrams were plotted using Grapher (8.0) software.

Several pollen indices have been designed to capture climate-related information for arid and semi-arid regions. For example, the ratio of Non-arboreal pollen to Arboreal pollen (NAP/AP) has been demonstrated to be an effective moisture index especially in sub-humid and semi-arid areas (Moore et al., 1991), and has been used in the Russian Altai Mountains (Blyakharchuk et al., 2007), the northern Mongolia (Dorofeyuk and Tarasov, 1998), and the Chinese Loess Plateau (Feng et al., 2004, 2006). SFI index (steppe-forest index = $[(\text{Artemisia} + \text{Chenopodiaceae} + \text{Ephedra} + \text{Caryophyllaceae}) / \text{Trees}]$) is the ratio of the main steppe pollen sum over the tree pollen sum and was used to reconstruct the areal extent of steppe expansion in Lake Hovsgol (Prokopenko et al., 2007). In addition, the $[C + A]/P$ ratio ($[(\text{Chenopodiaceae} + \text{Artemisia}) / \text{Poaceae}]$) was also designed to retrieve the Holocene aridity history in the Lake Telmen region of

central Mongolia (Fowell et al., 2003), though Poaceae has been demonstrated to be extremely under-represented in the pollen spectrum of the entire Mongolian Plateau (Gunin, 1999; Ma et al., 2008).

3.4. Vegetation and environmental reconstructions

The qualitative interpretation of pollen spectra can be checked with a quantitative method of pollen-based biome reconstruction (named Biomization, Prentice et al., 1996). Based on contemporary knowledge of the biogeography and ecology of modern plants, the pollen taxa are assigned to plant functional types (PFTs) and to main vegetation types (biomes) (Table 2). An affinity score for each single biome is then calculated according to Prentice et al. (1996). The pollen taxa-PFTs matrix applied in the present study is based on the Biomization procedure presented in Yu et al. (2000), but it was thoroughly improved by the information provided in Herzsuh et al. (2004) and Tarasov et al. (1998) (Table 2).

Table 2

Assignment of pollen taxa to the plant functional types (PFTs) for northern China (after Tarasov et al., 1998; Yu et al., (2000).

Abbreviation	Plant functional type	Pollen taxa
bec	Boreal evergreen conifer	<i>Abies</i> , <i>Picea</i>
bs	Boreal summergreen tree/shrub	<i>Betula</i> , <i>Salix</i>
ctc	Cool-temperate conifer	<i>Abies</i>
df	Desert forb/shrub	Asteraceae, Brassicaceae, Caryophyllaceae, Chenopodiaceae, Elaeagnaceae, <i>Ephedra</i> , Liliaceae, Polygonaceae, <i>Polygonum</i> , <i>Potentilla</i>
ec	Eurythermic conifer	<i>Pinus</i>
es	Eurythermic summergreen tree/shrub	<i>Alnus</i>
g	Grass	Poaceae
s	Sedge	Cyperaceae
sf	Steppe forb/shrub	Apiaceae, <i>Artemisia</i> , Asteraceae, Brassicaceae Caryophyllaceae, Chenopodiaceae, Elaeagnaceae, Fabaceae, Labiatae, Liliaceae, Moraceae, <i>Humulus</i> , <i>Plantago</i> , Polygonaceae, <i>Polygonum</i> , Thalictrum, Rosaceae, <i>Potentilla</i> , <i>Sanguisorba</i> , <i>Galium</i> , <i>Rumex</i> , <i>Urtica</i> , Valerianaceae
ts	Temperate summergreen tree/shrub	<i>Acer</i> , <i>Betula</i> , <i>Fraxinus</i> , <i>Quercus</i> , <i>Rubia</i> , <i>Salix</i>
ts1	Cool-temperate summergreen trees/shrub	<i>Carpinus</i> , <i>Corylus</i> , <i>Tilia</i> , <i>Ulmus</i>
ts2	Intermediate-temperate summergreen tree/shrub	<i>Celtis</i> , <i>Juglans</i> , <i>Pterocarya</i> , Thymelaceae

To reconstruct changes in palaeoclimatic parameters, PFT modern analogue technique (PFT-MAT) was applied. PFT-MAT method calculates a chord distance between the pollen taxa considered and modern analogues compared to determine the dissimilarity between the fossil and modern pollen spectra (Nakagawa et al., 2002; Davis et al., 2003; Jiang et al., 2006, 2009; Sun and Feng, 2013), which is constrained using modern pollen datasets and corresponding climatological data. The modern pollen dataset used in this study includes 1855 surface pollen spectra covering Mongolia and Europe (Guiot et al., 1993; Tarasov et al., 1998) and 211 surface pollen spectra from northern China provided by Members of China Quaternary Pollen Data Base (2001). The climate data of a specific surface pollen sample site are obtained using a weighted average of observed data from its adjacent weather stations within an area of $5 \times 5^\circ$ (Guiot and

Goery, 1996). For each fossil spectrum, we selected eight modern analogues with the smallest chord distance that represents the “best modern analogues”. The mean climate parameters of each fossil pollen assemblage are then calculated using the method described by Guiot et al. (1993) and Magny et al. (2001). All calculations were carried out using the PPPBASE software package (Guiot and Goery, 1996). We calculated three individual climatic parameters: the mean annual temperature (MAT), and mean annual precipitation (MAP).

4. Results

4.1. Fossil pollen data

Totally, 47 different types of terrestrial fossil pollen were identified from all samples analyzed in this study and they include 14 tree taxa and 33 herbaceous and shrub taxa (e.g., *Pinus*, *Picea*, Cupressaceae, *Betula*, *Quercus*, *Ulmus*, *Salix*, *Alnus*, *Corylus*, Rosaceae, *Ephedra*, *Nitraria*, *Tamarix*, Poaceae, *Artemisia*, Chenopodiaceae, Aster-type, *Taraxacum*-type, Anther-type, *Humulus*, Ranunculaceae, *Polygonum*, Cyperaceae, etc.). In addition, three aquatic pollen and two algae (e.g., *Typha*, *Sparganium*, *Alisma*; *Pediastrum* and *Myriophyllum*) were also identified. The core can be divided into three pollen assemblage zones and five subzones based on percentages of the major pollen taxa, and the three pollen zones and five subzones correspond well with the aforementioned sediment units (Fig. 3).

Pollen Zone 1 (200–172 cm; ~22,600–~13,200 cal BP) corresponds with the Sediment Unit 1 and the pollen assemblage is dominated by herb component (65–80%), mainly including Cyperaceae (12–35%), Poaceae (7–20%), Aster-type (3–6%), *Taraxacum* (2–8%), and Anther-type (1–10%). The coniferous tree component, including *Pinus* (10–20%), *Picea* (2–7%), Cupressaceae (0–7%) and *Larix* (0–2%), comprises ~20% of the total pollen sum. The broadleaved tree pollen percentage and pollen concentration are quite low. It should be mentioned that wetland taxa (e.g., Cyperaceae and *Typha*) percentages have the highest values of the entire core.

Pollen Zone 2 (172–112 cm; ~13,200–~6400 cal BP) corresponds with the Sediment Unit 2, 3, and 4, and is marked by a higher percentage of herbs and a relatively high pollen concentration. This zone can be further divided into three subzones.

Pollen subzone 2–1 (172–150 cm; ~13,200–~10,500 cal BP) corresponds with the Sediment Unit 2 and the pollen assemblage is dominated by herb and shrub components, mainly including *Artemisia* (35–45%), Chenopodiaceae (20–30%), Poaceae (8–17%) and *Ephedra* (1–8%). The coniferous tree component abruptly decreased (<10%) and mainly includes *Pinus*, *Picea*, and Cupressaceae. Broadleaved tree pollen started to emerge and main pollen types are *Quercus*, *Betula*, *Populus*, and *Ulmus*. Pollen subzone 2–2 (150–130 cm; ~10,500–~8900 cal BP) corresponds with the Sediment Unit 3. Compared with Pollen subzone 2–1, Poaceae and *Betula* pollen percentages and pollen concentration increased while *Ephedra* pollen percentages decreased in pollen subzone 2–2. Pollen subzone 2–3 (130–112 cm; ~8900–~6400 cal BP), corresponding with the Sediment Unit 4, is distinctively characterized by dramatic increases in drought-tolerant shrubs (e.g., *Ephedra*) and also by dramatic decreases in pollen concentration. The *Pinus* pollen percentage gradually increased.

Pollen Zone 3 (112–0 cm; ~6400–~0 cal BP) corresponds with the Sediment Unit 5. The assemblage is marked by increased coniferous (up to 45%) and broadleaved tree pollen percentages (up to 10%) at the expense of the herb pollen percentage (50–70%). The coniferous trees are mainly *Pinus* (20–35%), *Picea* (1–5%), Cupressaceae (0–9%) and *Larix* (0–5%), and *Pinus* is the major contributor to the increase in the coniferous tree pollen percentage. The

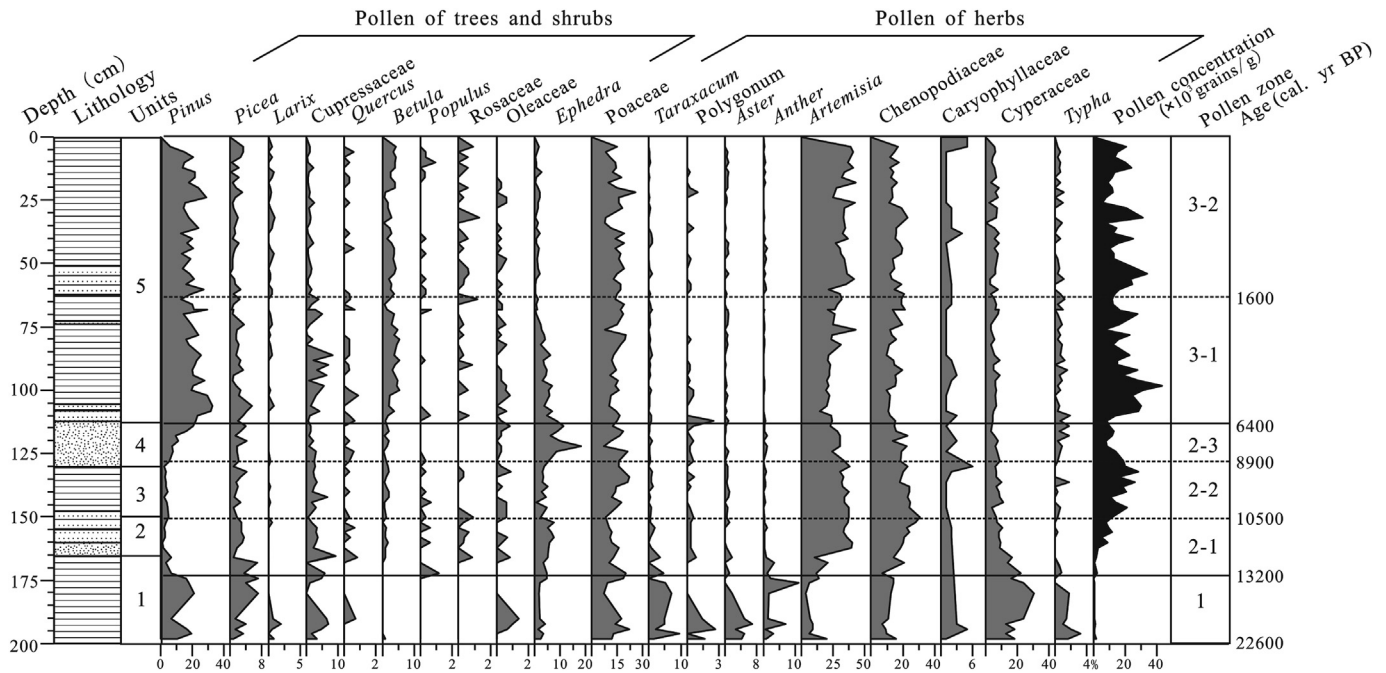


Fig. 3. Pollen spectra and taxa percentages of Achit Nur core.

broadleaved trees are mainly *Betula* (2–6%), *Populus* (0–2%) and *Quercus* (0–1%). The pollen concentration increased significantly compared with the underlying Pollen subzone 2–3. This zone can also be divided into two subzones. Compared with pollen subzone 3–2 (62–0 cm; ~1600–~0 cal BP), pollen subzone 3–1 (112–62 cm; ~6400–~1600 cal BP) has higher tree pollen percentages (e.g., *Pinus*, *Picea*, Cupressaceae, *Betula*) and higher pollen concentration (the mean value is $\sim 20 \times 10^3$ grains/g).

4.2. Vegetation and environmental reconstructions

The qualitative interpretation of the vegetation history of Achit Nur is in concordance with that reconstructed by the quantitative method of biomization. Fig. 4 shows that biome types of the highest scores at each level are associated with a greater likelihood of that vegetation type being present near the site. The method of biomization and the taxa-biome matrix used here do not allow the

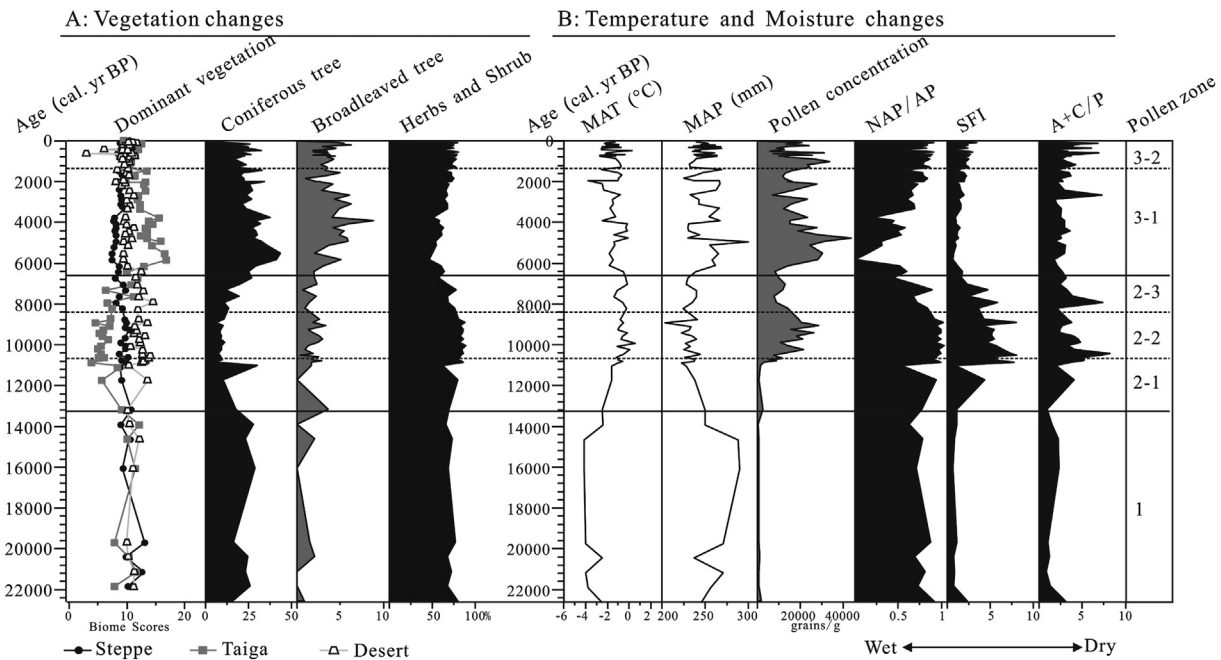


Fig. 4. Vegetation and environmental reconstructions. A: Vegetation changes, including dominant vegetation by biomization reconstructed, pollen percentages of coniferous tree, broadleaved tree, and herbs and shrub. B: Temperature and Moisture changes, including the reconstructed results of MAT, MAP, pollen concentration, NAP/AP ratio, SFI index, and [A + C]/P ratio. AP: Arboreal pollen; NAP: Non-arboreal pollen; SFI: steppe-forest index=(*Artemisia* + *Chenopodiaceae* + *Ephedra* + *Caryophyllaceae*)/Trees; A: *Artemisia*; C: *Chenopodiaceae*; P: *Poaceae*.

reconstruction of transitional vegetation types (e.g., forest-steppe or desert-steppe). However, additional information can be obtained by examining the relative values of forest and non-forest biome scores. The scores for steppe are close to those for taiga in the bottom part (~22,600–~13,200 cal BP) and top part (~1600–~0 cal BP) of the Achit Nuur record, probably suggesting a forest-steppe transitional vegetation. The scores for desert are close to those for steppe during the period between ~13,200 and ~6400 cal BP, most likely indicating a desert-steppe transitional vegetation. The vegetation reconstructed for the period between ~6400 and ~1600 cal BP is a taiga. The reconstructed biome types are relatively well corroborated by main pollen assemblage (e.g., percentages of coniferous trees, broadleaved trees and Herbs) (Fig. 4).

Our reconstruction of MAT was well identified the cold climates during Last Glacial Maximum and the subsequent late glacial from ~22,600 to ~13,200 cal BP. A general warming between ~13,200 and ~10,500 cal BP was also well-displayed, being relatively consistent with the records from North Atlantic region (Davis et al., 2003; Moros et al., 2004). The highest values of the reconstructed MAT well marked the early-middle Holocene “hyperthermal period” lasting from ~10,500–~6400 cal BP (Harrison et al., 1996; Tarasov et al., 2000; Rudaya et al., 2009) and the fluctuating decline of the reconstructed MAT characterized the following period from ~6400 to ~2000 cal BP, being supportive to the cooling of large-scale (Wanner et al., 2008). It seems that the slight warming of the past ~1000 years reported from the Western Pacific Warm Pool (Stott et al., 2004) and also from the Arabian Sea of the Indian Ocean (Gupta et al., 2003) were also captured in our record from Achit Nuur (Fig. 4). The reconstructed MAP exhibits two wet periods: (1) from ~22,600 to ~13,200 cal BP and (2) from ~6400 to ~1600 cal BP. The two intervening dry periods are: (1) from ~13,200–~6400 cal BP and (2) from ~1600 to 0 cal BP.

5. Discussion and conclusions

5.1. Vegetation variations and associated climate changes

The pollen assemblage of Achit Nuur sediment core reveals a detailed history of changes in the vegetation and climate over the Achit Nuur area during the last ~22,600 y (Figs. 3 and 4). The highest values of wetland taxa (e.g., Cyperaceae, *Typha*) percentages showed that the lake basin was dominated by meadow-steppe between ~22,600 and ~13,200 cal BP, suggesting that the moisture was high. This reconstructed high moisture is corroborated by the lowest values of SFI scores and $[A + C]/P$ ratios. A higher percentage of coniferous tree pollen suggested that the dark-coniferous forests expanded in the surrounding mountains compared with the subsequent stages. It can thus be inferred that the climate was cold and humid during the period from ~22,600 to ~13,200 cal BP.

The vegetation was desert-steppe dominated by *Artemisia*, Chenopodiaceae, Poaceae, and *Ephedra*, as shown by the high herb pollen sum, high SFI scores and high $[A + C]/P$ ratios during the period from ~13,200–~6400 cal BP, meaning that the climate in this region is mild and dry and the lake level declined. All data (including MAT, MAP, NAP/AP ratio, $[A + C]/P$ ratio, and SFI score) indicated that the moisture level was the lowest and the temperature was the highest between 10,500 and 6400 cal BP.

The biomization reconstruction shows that Taiga vegetation in high elevations and deciduous forest in medium elevations expanded in the surrounding mountains as indicated by increased pollen percentages of coniferous and broadleaved trees between ~6400 and ~1600 cal BP. The expansion of forests in the surrounding mountains and lowered values in the NAP/AP ratio and SFI

score all suggested that the moisture level was increased under declined temperature conditions. Since ~1600 cal BP, steppe vegetation recovered in the lake basin and the climate became drier than the previous stage under increased temperature conditions, as indicated by increases in NAP/AP ratio, $[A + C]/P$ ratio and SFI scores.

5.2. Regional comparison

To understand the Holocene vegetation and climate history of the western Mongolian Plateau in a large-scale geographic context, the following section will focus on the issues surrounding the Holocene pollen records. We chose five sections from three surrounding areas in hope that our understanding of the large-scale controlling mechanisms can be improved. These five sections are Ugii Nuur, Lake Telmen, and Lake Hovsgol in the northern Mongolian Plateau, Hoton Nuur in the northern part of the Altai Mountain, and Lake Wulungu in northern Xinjiang.

Ugii Nuur (site 2 in Fig. 1) (Wang et al., 2009, 2011), Lake Telmen (site 3 in Fig. 1) (Peck et al., 2002; Fowell et al., 2003), and Lake Hovsgol (site 4 in Fig. 1) (Prokopenko et al., 2007) are situated in the northern Mongolian Plateau. Multi-proxy reconstruction from Ugii Nuur shows that a mild climate with moderate moisture conditions supported a desert steppe landscape during ~9100–6700 cal BP, followed by a mid-Holocene dry phase lasting from ~6700 to 3300 cal BP. The changes in Chenopodiaceae percentage and pollen-based moisture index exhibit a wet period between ~2600 and 1000 cal BP that was followed by a relatively dry period (i.e., the past ~1000 years). The pollen-based aridity index (i.e., $[A + C]/P$) from Lake Telmen (Peck et al., 2002; Fowell et al., 2003) exhibits a mid-Holocene dry phase lasting from 7100 to 4600 cal BP, which is generally supportive to the mid-Holocene dry phase reconstructed at Ugii Nuur. The following period, from ~4600 to 0 cal BP, has been generally wet with two short dry intervals at ~3000 and at ~1800 cal BP. At Lake Hovsgol (Prokopenko et al., 2007), the pollen-based steppe-forest index (i.e., SFI index) indicated a wet condition from ~9500 to ~6000 cal BP, a mid-Holocene dry phase from ~6000 to ~3500 cal BP, and a relatively wet phase after ~3500 cal BP. On the whole, above three pollen records from the northern Mongolian Plateau suggest that the climate was mild and wet during the early Holocene (~9500–~7000 cal BP) and the late Holocene (after ~3500 cal BP), but dry during the middle Holocene (~7000–~3500 cal BP).

A newly recovered sequence from Hoton Nuur (site 5 in Fig. 1) (Rudaya et al., 2009) within the Mongolian Altai area significantly improved the sampling resolution over the old sequence reported by Tarasov et al. (2000). The pollen-based quantitative reconstruction of precipitation using the best modern analogue technique suggests that the regional climate was relatively dry prior to 10,500 cal BP and became substantially wetter during the following interval between 10,500 and 5000 cal BP. Pollen data and biome reconstruction demonstrate that a cool steppe predominated around Hoton Nuur before 10,500 cal BP, followed by the spread of boreal trees and open woodland vegetation between 10,500 and 6500 cal BP. From 6500 cal BP onward, steppe taxa in the pollen spectra increase significantly, indicating a strengthening of steppe communities and a weakening of taiga communities.

Wulungu Lake in northern Xinjiang (Xiao et al., 2006; Liu et al., 2008) (site 6 in Fig. 1) had experienced a shallow lake or wetland environment during the early Holocene (~10,000–6700 cal BP) as indicated by high pollen-based wetland biome scores (Xiao et al., 2006; Liu et al., 2008). A general wetting trend since 6700 cal BP is suggested by an increasing of A/C ratio and a decreasing of pollen-based desert biome scores, suggesting that the Holocene moisture optimum occurred between 4200 and 500 cal BP (Liu et al., 2008).

To sum up, in the arid areas of the northern Mongolian Plateau (e.g., Ugii Nuur, Lake Telmen, and Lake Hovsgol), a mid-Holocene dry phase can be established, and both the early Holocene and the late Holocene are characterized by relatively wet (and probably also cool) climates. In the Mongolian Altai area (e.g., Hoton Nuur), the regional climate was relatively dry prior to 10,500 cal BP and became substantially wetter during the following interval between 10,500 and 5000 cal BP. A drying trend over the past ~5000 years is well expressed by all pollen proxies. In the northern Xinjiang, a dry early Holocene and a progressively wetter middle and late Holocene pattern can be established for Lake Wulungu.

The record covering the past ~22,600 years from Achit Nuur in the western Mongolian Plateau seems in a good agreement with large-scale picture of climate change during the same period, somewhat boosting our confidence on our reconstructions. However, the Holocene part of the record from Achit Nuur does not correlate with the records from nearby Hoton Nuur and from Wulungu Lake. Instead, the Holocene part of the record from Achit Nuur is more or less consistent with the records from the northern Mongolian Plateau (including Ugii Nuur, Lake Telmen, and Lake Hovsgol), seemingly lending support to the proposition that the moisture levels in arid and hyper-arid areas of the Mongolian Plateau has been primarily controlled or modulated by temperature (Wang et al., 2009, 2011; Wang and Feng, 2013). The proposition states that the elevated temperature resulted in an increase in evaporation and thus led to a decrease in moisture level. This inference is generally supported by qualitative (e.g., pollen assemblages) and semi-quantitative (e.g., pollen ratios and biome scores) reconstructions reconstruction from Achit Nuur. The dilemma we have to face is that the reconstructed MAP goes along with the qualitatively and semi-quantitatively reconstructed moisture levels, severely undermining the proposition that temperature has controlled or modulated the moisture levels. However, if the reconstructions of MAT and MAP can stand for further tests, the climate change in Achit area seems to have followed cool-wet mode and warm-dry mode, a typical temperature-precipitation combination for the westerlies-dominated climate (Aizen et al., 2001; Bridgman and Oliver, 2006; Bothe et al., 2011).

5.3. A brief summary

During the period of ~22,600–~13,200 cal BP, the vegetation of the Achit Nuur region was forests and steppes. That is, steppes dominated the lake basin and cold-tolerant forests dominated the surrounding mountains, suggesting a cold and wet climate. Subsequently from ~13,200 to ~6400 cal BP, deserts in lower elevations and steppes in higher elevations developed under mild and dry conditions in the Achit area. Taiga vegetation expanded in the surrounding mountains under cooling and humid conditions from ~6400 to ~1600 cal BP and forests and steppes resumed over the past ~1600 years.

Pollen-based biomization and PFT-MAT quantitative reconstruction demonstrate that: (1) temperature and moisture have changed asynchronously during the last glacial, (2) the warmest period occurred between ~10,500 and ~7000 cal BP and the most humid period occurred between ~22,600 and ~13,200 cal BP, and (3) higher temperatures may have brought not only more precipitation, but also more evaporation, thereby resulting in dry climates between ~13,200 and ~6400 cal BP.

Acknowledgments

This study was financially supported by several NSFC grants (No. 40930120, No. 41002058, No. 41172332, No. 40331012, No.

40421101) and two U.S. NSF grants (NSF-ESH-04-02509, NSF-BSC-06-52304).

References

- Aizen, E.M., Aizen, V.B., Melack, J.M., Nakamura, T., Ohta, T., 2001. Precipitation and atmospheric circulation patterns at mid-latitudes of Asia. *International Journal of Climatology* 21, 535–556.
- Blyakharchuk, T.A., Wright, H.E., Borodavko, P.S., van der Knaap, W.O., Ammann, B., 2007. Late Glacial and Holocene vegetational history of the Altai Mountains (southwestern Tuva Republic, Siberia). *Palaeogeography, Palaeoclimatology, Palaeoecology* 245, 518–534.
- Bothe, O., Fraedrich, K., Zhu, X., 2011. Precipitation climate of Central Asia and the large-scale atmospheric circulation. *Theoretical Applied Climatology*. <http://dx.doi.org/10.1007/s00704-011-0537-2>.
- Bridgman, B.H., Oliver, J.E., 2006. *The Global Climate System: Patterns, Processes, and Teleconnections*. Cambridge University Press, New York, p. 243.
- Chen, F.H., Yu, Z.C., Yang, M.L., Ito, E., Wang, S.M., Madsen, D.B., Huang, X.Z., Zhao, Y., Sato, T., Birks, H.J.B., Boomer, I., Chen, J.H., An, C.B., Wünnemann, B., 2008. Holocene moisture evolution in arid central Asia and its out-of-phase relationship with Asian monsoon history. *Quaternary Science Reviews* 27 (3–4), 351–364.
- Davis, B.A.S., Brewer, S., Stevenson, A.C., Guiot, J., Data, Contributors, 2003. The temperature of Europe during the Holocene reconstructed from pollen data. *Quaternary Science Reviews* 22, 1701–1716.
- Dorofeyuk, N.I., Tarasov, P.E., 1998. Vegetation and lake levels in Northern Mongolia in the last 12,500 years as indicated by data of pollen and diatom analyses. *Stratigraphy and Geological Correlation* 6 (1), 70–83.
- Erdtman, G., 1978. *Handbook of Palynology* (Translated by the Institute of Botany, the Chinese Academy of Sciences). Science Press, Beijing (in Chinese).
- Feng, Z.D., An, C.B., Tang, L.Y., Jull, A.J.T., 2004. Stratigraphic evidence of a Mega-humid climate between 10,000 and 4000 years B.P. in the western part of the Chinese Loess Plateau. *Global and Planetary Change* 43 (3–4), 145–155.
- Feng, Z.D., Tang, L.Y., Wang, H.B., Ma, Y.Z., Liu, K.B., 2006. Holocene vegetation variations and the associated environmental changes in the western part of the Chinese Loess Plateau. *Palaeogeography, Palaeoclimatology, Palaeoecology* 241, 440–456.
- Fowell, S.J., Hansen, B., Peck, J.A., Khosbayan, P., Ganbold, E., 2003. Mid to late Holocene climate evolution of the Lake Telmen basin, north central Mongolia, based on palynological data. *Quaternary Research* 59 (3), 353–363.
- Grunert, J., Lehmkuhl, F., Walthert, M., 2000. Paleoclimatic evolution of the Uvs Nuur basin and adjacent areas (Western Mongolia). *Quaternary International* 65/66, 171–191.
- Guiot, J., Harrison, S.P., Prentice, T.C., 1993. Reconstruction of Holocene patterns of moisture in Europe using pollen and lake-level data. *Quaternary Research* 40, 139–149.
- Guiot, J., Goeury, C., 1996. PPPBASE, a software for statistical analysis of paleoecological and paleoclimatological data. *Dendrochronologia* 14, 295–300.
- Gunin, P.D., 1999. *Vegetation Dynamics of Mongolia*. Kluwer Academic Publisher, Copenhagen, p. 238.
- Gupta, A.K., Anderson, D.M., Overpeck, J.T., 2003. Abrupt changes in the Asian southwest monsoon during the Holocene and their links to the North Atlantic Ocean. *Nature* 421, 354–357.
- Harrison, S.P., Yu, G., Tarasov, P.E., 1996. Late Quaternary lake-level record from Northern Eurasia. *Quaternary Research* 45 (2), 138–159.
- Herzschuh, U., Tarasov, P., Wünnemann, B., Hartmann, K., 2004. Holocene vegetation and climate of the Alashan Plateau, NW China, reconstructed from pollen data. *Palaeogeography Palaeoclimatology Palaeoecology* 211 (1–2), 1–17.
- Hilbig, W., 1995. *The Vegetation of Mongolia*. SPB Academic Publishing, Amsterdam, p. 258.
- Jiang, W.Y., Guo, Z.T., Sun, X.J., Wu, H.B., Chu, G.Q., Yuan, B.Y., Hatté, C., Guiot, J., 2006. Reconstruction of climate and vegetation changes of Lake Bayanchagan (Inner Mongolia): Holocene variability of the East Asian monsoon. *Quaternary Research* 65 (3), 411–420.
- Jiang, W.Y., Guiot, J., Chu, G.Q., Wu, H.B., Yuan, B.Y., Hatté, C., Guo, Z.T., 2009. An improved methodology of the modern analogues technique for palaeoclimate reconstruction in arid and semi-arid regions. *Boreas* 39, 145–153.
- Liu, X.Q., Herzschuh, U., Shen, J., Jiang, Q.F., Xiao, X.Y., 2008. Holocene environmental and climatic changes inferred from Wulungu Lake in northern Xinjiang, China. *Quaternary Research* 70 (3), 412–425.
- Ma, Y.Z., Liu, K.-B., Feng, Z.D., Sang, Y.L., Wang, W., Sun, A.Z., 2008. A survey of modern pollen and vegetation along a south–north transect in Mongolia. *Journal of Biogeography* 35, 1512–1532.
- Magny, M., Guiot, J., Schoellammer, P., 2001. Quantitative reconstruction of Younger Dryas to Mid-Holocene paleoclimates at Le Locle, Swiss Jura, using pollen and lake-level data. *Quaternary Research* 56, 170–180.
- Members of China Quaternary Pollen Data Base, 2001. Simulation of China biome reconstruction based on pollen data from surface sediment samples. *Acta Botanica Sinica* 43, 201–209.
- Moore, P.D., Web, J.A., 1987. *Palynology Analytical Manual* (Li WY, Xiao XM, Liu GX Trans.). Guangxi People's Publishing House, Nanning (in Chinese).
- Moore, P.D., Webb, J.A., Collinson, M.E., 1991. *Pollen Analysis*, second ed. Blackwell Scientific Publication, Oxford, p. 216.

- Moros, M., Emeis, K., Risebrobakken, B., Snowball, I., Kuipers, A., McManus, J., Jansen, E., 2004. Sea surface temperature and ice rafting in the Holocene North Atlantic: climate influences on northern Europe and Greenland. *Quaternary Science Reviews* 23, 2113–2160.
- Nakagawa, T., Tarasov, P.E., Nishida, K., Gotanda, K., Yasuda, Y., 2002. Quaternary pollen-based climate reconstruction in central Japan: application to surface and Late Quaternary spectra. *Quaternary Science Reviews* 21, 2099–2113.
- Peck, J.A., Khosbayan, P., Fowell, S.J., Pearce, R.B., Ariunbileg, S., Hansen, B., Soninkhishig, N., 2002. Mid to Late Holocene climate change in north central Mongolia as recorded in the sediments of Lake Telmen. *Palaeogeography Palaeoclimatology Palaeoecology* 183 (1–2), 135–153.
- Prentice, I.C., Guiot, J., Huntley, B., Jolly, D., Cheddadi, R., 1996. Reconstructing biomes from palaeoecological data: a general method and its application to European pollen data at 0 and 6 ka. *Climate Dynamics* 12, 185–194.
- Prokopenko, A.A., Alexander, A., Khursevich, G.K., Bezrukova, E.V., Kuzmin, M.I., Boes, X., Williams, D.F., Fedenya, S.A., Kulagina, N.V., Letunova, P.P., Abzaeva, A.A., 2007. Paleoenvironmental proxy records from Lake Hovsgol, Mongolia, and a synthesis of Holocene climate change in the Lake Baikal watershed. *Quaternary Research* 68 (1), 2–17.
- Reimer, P.J., Baillie, M.G.L., Bard, E., Bayliss, A., Beck, J.W., Blackwell, P.G., Ramsey, C.B., Buck, C.E., Burr, G.S., Edwards, R.L., et al., 2009. IntCal09 and Marine09 radiocarbon age calibration curves, 0–50,000 years cal BP. *Radiocarbon* 51, 1111–1150.
- Rudaya, N., Tarasov, P., Dorofeyuk, N., Solovieva, N., Kalugin, I., Andreev, A., Daryin, A., Diekmann, B., Riedel, F., Tserendash, N., Wagner, M., 2009. Holocene environments and climate in the Mongolian Altai reconstructed from the Hoton-Nur pollen and diatom records: a step towards better understanding climate dynamics in Central Asia. *Quaternary Science Reviews* 28 (5–6), 540–554.
- Stott, L., Cannariato, K., Thunell, R., Haug, G.H., Koutavas, A., Lund, S., 2004. Decline of surface temperature and salinity in the western tropical Pacific Ocean in the Holocene epoch. *Science* 431, 56–59.
- Sun, A.Z., Feng, Z.D., 2013. Holocene climatic reconstructions from the fossil pollen record at Qigai Nuur in the southern Mongolian Plateau. *The Holocene*. <http://dx.doi.org/10.1177/0959683613489581>.
- Tarasov, P., Dorofeyuk, N., Metl'tseva, E., 2000. Holocene vegetation and climate changes in Hoton-Nur basin, northwest Mongolia. *Boreas* 29 (2), 117–126.
- Tarasov, P.E., Webb II, I.T., Andreev, A.A., Afanas'eva, N.B., Berezina, N.A., Blyakharchuk, T.A., Bolikhovskaya, N.S., Cheddadi, R., Chernavskaya, M.M., Chernova, G.M., et al., 1998. Present-day and mid-Holocene biomes reconstructed from pollen and plant macrofossil data from the former Soviet Union and Mongolia. *Journal of Biogeography* 25, 1029–1053.
- Wang, F.X., Qian, N.F., Zhang, Y.L., Yang, H.U., 1995. *Pollen Flora of China*, second ed. Science Press, Beijing. (in Chinese).
- Wang, W., Feng, Z.-D., 2013. Holocene moisture evolution across the Mongolian Plateau and its surrounding areas: a synthesis of climatic records. *Earth-Science Reviews* 122, 38–57.
- Wang, W., Ma, Y.Z., Feng, Z.D., Meng, H.W., Sang, Y.L., Zhai, X.W., 2009. Vegetation and climate changes during the last 8660 cal. a BP in central Mongolia, based on a high-resolution pollen record from Lake Ugii Nuur. *Chinese Science Bulletin* 54 (9), 1579–1589.
- Wang, W., Ma, Y.Z., Feng, Z.D., Narantsetseg, Ts., Liu, K.B., Zhai, X.W., 2011. A prolonged dry mid-Holocene climate revealed by pollen and diatom records from Lake Ugii Nuur in central Mongolia. *Quaternary International* 229 (1–2), 74–83.
- Wanner, H., Beer, J., Bütikofer, J., Crowley, T.J., Cubasch, U., Flückiger, J., Gose, H., Grosjean, M., Joos, F., Kaplan, J.O., Küttel, M., Müller, S.A., Prentice, I.C., Solomina, O., Stocker, T.F., Tarasov, P., Wagner, M., Widmann, M., 2008. Mid- to Late-Holocene climate change: an overview. *Quaternary Science Reviews* 267, 1791–1828.
- Xiao, X.Y., Jiang, Q.F., Liu, X.Q., Xiao, H.F., Shen, J., 2006. High resolution sporopollen record and environmental change since Holocene in the Wulungu Lake, Xinjiang. *Acta Micropalaeontologica Sinica* 23 (1), 77–86 (in Chinese with English Abstract).
- Yu, G., Chen, X.D., Ni, J., Cheddadi, R., Guiot, J., Han, H., Harrison, S.P., Huang, C., Ke, M., Kong, Z., Li, S., Li, W., Liew, P., Liu, G., Liu, Q., Liu, K.-B., et al., 2000. Palaeovegetation of China: a pollen data-based synthesis for the mid-Holocene and last glacial maximum. *Journal of Biogeography* 27, 635–664.